Tight framelets on graphs for multiscale data analysis

Yu Guang Wang[a] and Xiaosheng Zhuang[b]

[a]School of Mathematics and Statistics, the University of New South Wales, Sydney, Australia
[b]Department of Mathematics, City University of Hong Kong, Kowloon Tong, Hong Kong

ABSTRACT

In this paper, we discuss the construction and applications of *decimated tight framelets* on graphs. Based on graph clustering algorithms, a coarse-grained chain of graphs can be constructed where a suitable orthonormal eigen-pair can be deduced. Decimated tight framelets can then be constructed based on the orthonormal eigen-pair. Moreover, such tight framelets are associated with filter banks with which fast framelet transform algorithms can be realized. An explicit toy example of decimated tight framelets on a graph is provided.

Keywords: Tight framelets, framelets on graphs, decimated framelets, graph signal processing, filter banks, fast algorithms, fast framelet transforms, coarse-grained chain, spectral graph theory, graph Laplacian.

1. INTRODUCTION

On Euclidean domains, harmonic analysis has been an active research branch of mathematics since the work of Fourier. In the past two centuries, it has become a vast subject with applications in areas as diverse as signal processing, representation theory, number theory, quantum mechanics, tidal analysis and neuroscience. In the last four decades, one of its sub-branches, called wavelet analysis, has been intensively studied and well developed by many pioneered as well as currently active researchers.[1–5] In recent years, there has been a great interest in developing wavelet-like representation systems for data defined on non-Euclidean domains, including manifolds and graphs. One of the motivations is from the interdisciplinary area of machine learning, where data concerned are massive and typically from social networks, biology, physics, finance, etc., which can be naturally organized as graphs or graph data. Such 'Big Data' can be regarded as random samples from some smooth manifold, where its 'graph Laplacian' is connected to the 'manifold Laplacian'[6] encoding the essential information of the data to be exploited by various machine/deep learning approaches.[7–9]

In this paper, we focus on the construction of wavelet-like representation systems (framelets or wavelet frames) on graphs for Graph Signal Processing (GSP). Based on sequences of affine systems, we construct *decimated tight framelets* on a graph and provide discrete framelet transforms (*decomposition* and *reconstruction*) on graph for GSP.

2. DECIMATED TIGHT FRAMELETS ON A GRAPH

In this section, we investigate the characterization and construction of *decimated tight framelets* on a graph $\mathcal{G}$.

2.1 Graphs, chains, and orthonormal bases

An *undirected and weighted graph* $\mathcal{G}$ is an ordered triple $\mathcal{G} = (V, E, \boldsymbol{w})$ with a non-empty finite set V of *vertices*, a set $E \subseteq V \times V$ of *edges* between vertices in V, and a non-negative *weight function* $\boldsymbol{w} : E \to \mathbb{R}$. We denote $|V|$ and $|E|$ the number of vertices and edges. An edge $e \in E$ with vertices $p, v \in V$ is an unordered pair denoted by (p, v) or (v, p). We extend $\boldsymbol{w}$ from E to $V \times V$ by $\boldsymbol{w}(p, v) := 0$ for $(p, v) \notin E$. Note that for an undirected graph, the weight $\boldsymbol{w}$ is *symmetric* in the sense that $\boldsymbol{w}(p, v) = \boldsymbol{w}(v, p)$ for all $p, v \in V$. The *degree* of a vertex $v \in V$, denoted as $\boldsymbol{d}(v)$, is $\boldsymbol{d}(v) := \sum_{p \in V} \boldsymbol{w}(v, p)$. We denote $\mathrm{vol}(\mathcal{G}) := \mathrm{vol}(V) = \sum_{v \in V} \boldsymbol{d}(v)$ the volume of the graph, which is the sum of degrees of all vertices of $\mathcal{G}$. Throughout the paper, we only consider *connected* graphs, where between any two vertices there exists a path.

Send correspondence to X. Zhuang (xzhuang7@cityu.edu.hk), Phone: +852 3442 5942. Further author information: Y. G. Wang (yuguang.wang@unsw.edu.au).

Let $\mathcal{G} = (V, E, \boldsymbol{w})$ and $\mathcal{G}_c = (V_c, E_c, \boldsymbol{w}_c)$ be two graphs. We say that $\mathcal{G}_c$ is the *coarse-grained graph* of $\mathcal{G}$ if V_c is a *partition* of V; i.e., there exists subsets $V_1, \ldots, V_k$ of V for some $k \in \mathbb{N}$ such that

$$V_c = \{V_1, V_2, \ldots, V_k\}, \quad V_1 \cup \cdots \cup V_k = V, \quad V_i \cap V_j = \emptyset, \quad 1 \le i < j \le k.$$

In such a case, each vertex V_j of $\mathcal{G}_c$ is called a *cluster* for $\mathcal{G}$. The edges of $\mathcal{G}_c$ are edges between clusters of $\mathcal{G}$. Clusters in $\mathcal{G}_c$ define an *equivalence relation* on $\mathcal{G}$: two vertices $p, v \in \mathcal{G}$ are equivalent, denoted by $p \sim v$, if p and v belong to the same cluster. An equivalent class (cluster) in $\mathcal{G}$, which is a vertex in $\mathcal{G}_c$, associated with a vertex $v \in V$ can then be denoted as $[v]_{\mathcal{G}_c} := \{p \in \mathcal{G} : p \sim v\}$, and we have $V_c = V/\!\sim\, = \{[v]_{\mathcal{G}_c} : v \in V\}$. If no confusion arises, we will drop the subscript $\mathcal{G}_c$ and simply use $[v]$ to denote a cluster in $\mathcal{G}$ with respect to the coarse-grained graph $\mathcal{G}_c$. Note that a vertex $v \in \mathcal{G}$ can be viewed as $[v]_{\mathcal{G}} = \{v\}$, which is a singleton.

Given a graph $\mathcal{G} = (V, E, \boldsymbol{w})$, there are tremendous many clustering algorithms to obtain clusters of $\mathcal{G}$, either spectral[10–12] or non-spectral[13–17] based. For example, the NHC algorithm[18] is a non-spectral algorithm for clustering. Once we obtain clusters $\{V_1, \ldots, V_k\} =: V_c$ from $\mathcal{G}$, we can define[17] a weight function $\boldsymbol{w}_c$ on $V_c \times V_c$ by

$$\boldsymbol{w}_c([p], [v]) := \sum_{p \in [p]} \sum_{v \in [v]} \frac{\boldsymbol{w}(p, v)}{\mathrm{vol}(\mathcal{G})}, \quad [p], [v] \in V_c, \tag{1}$$

which determines an (undirected) edge set E_c by $E_c := \{([p], [v]) : \boldsymbol{w}_c([p], [v]) > 0\}$. The new graph $\mathcal{G}_c := (V_c, E_c, \boldsymbol{w}_c)$ is then a coarse-grained graph of $\mathcal{G}$. Recursively doing this step, we would obtain a *chain* of graphs from the original graph $\mathcal{G}$. More precisely, let $J \ge J_0$ be two integers. We say that the sequence $\mathcal{G}_{J \to J_0} := (\mathcal{G}_J, \mathcal{G}_{J-1}, \ldots, \mathcal{G}_{J_0})$ with $\mathcal{G}_J \equiv \mathcal{G}$ is a *coarse-grained chain* of $\mathcal{G}$ if $\mathcal{G}_j = (V_j, E_j, \boldsymbol{w}_j)$ is a coarse-grained graph of $\mathcal{G}$ for all $J_0 \le j \le J$ and $[v]_{\mathcal{G}_j} \subseteq [v]_{\mathcal{G}_{j-1}}$ for all $j = J, \ldots, J_0 + 1$ and for all $v \in V$. Note that, we treat each vertex v of the finest level graph $\mathcal{G}_J \equiv \mathcal{G}$ as a cluster of singleton. See Figure 3 for an illustration of a coarse-grained chain.

By $L_2(\mathcal{G}) := L_2(\mathcal{G}, \langle \cdot, \cdot \rangle_{\mathcal{G}})$, we denote the Hilbert space of *vectors* $\boldsymbol{f} : V \to \mathbb{C}$ on the graph $\mathcal{G}$ equipped with the inner product $\langle \cdot, \cdot \rangle_{\mathcal{G}}$:

$$\langle \boldsymbol{f}, \boldsymbol{g} \rangle_{\mathcal{G}} := \sum_{v \in V} \boldsymbol{f}(v) \overline{\boldsymbol{g}(v)}, \quad \boldsymbol{f}, \boldsymbol{g} \in L_2(\mathcal{G}),$$

where $\overline{\boldsymbol{g}}$ is the complex conjugate to $\boldsymbol{g}$. The induced norm $\|\cdot\|_{\mathcal{G}}$ is then given by $\|\boldsymbol{f}\|_{\mathcal{G}} := \sqrt{\langle \boldsymbol{f}, \boldsymbol{f} \rangle_{\mathcal{G}}}$ for $\boldsymbol{f} \in L_2(\mathcal{G})$. For simplicity, we shall drop the subscript $\mathcal{G}$, and simply use $\langle \cdot, \cdot \rangle$ and $\|\cdot\|$. Let $N := |V|$. A set $\{\boldsymbol{u}_\ell\}_{\ell=1}^N$ of vectors in $L_2(\mathcal{G})$ is an *orthonormal basis* for $L_2(\mathcal{G})$ if

$$\langle \boldsymbol{u}_\ell, \boldsymbol{u}_{\ell'} \rangle = \delta_{\ell, \ell'}, \quad 1 \le \ell, \ell' \le N,$$

where $\delta_{\ell,\ell'}$ is the *Kronecker delta* satisfying $\delta_{\ell,\ell'} = 1$ if $\ell = \ell'$ and 0 otherwise.

We say that $\{(\boldsymbol{u}_\ell, \lambda_\ell)\}_{\ell=1}^N$ is an *orthonormal eigen-pair* for $L_2(\mathcal{G})$ if $\{\boldsymbol{u}_\ell\}_{\ell=1}^N$ is an orthonormal basis for $L_2(\mathcal{G})$ with $\boldsymbol{u}_1 \equiv \frac{1}{\sqrt{N}}$ and $\{\lambda_\ell\}_{\ell=1}^N \subseteq \mathbb{R}$ is a nondecreasing sequence of nonnegative numbers satisfying $0 = \lambda_1 \le \cdots \le \lambda_N$. A typical example of orthonomral eigen-pairs is the set of pairs of the eigenvectors and eigenvalues of the (combinatorial or unnormalized) *graph Laplacian* $\mathcal{L} : L_2(\mathcal{G}) \to L_2(\mathcal{G})$ defined by

$$[\mathcal{L}\boldsymbol{f}](p) := \boldsymbol{d}(p)\boldsymbol{f}(p) - \sum_{v \in V} \boldsymbol{w}(p, v)\boldsymbol{f}(v), \quad p \in V, \boldsymbol{f} \in L_2(\mathcal{G}). \tag{2}$$

One can verify that $\langle \boldsymbol{f}, \mathcal{L}\boldsymbol{f} \rangle = \frac{1}{2} \sum_{p,v} \boldsymbol{w}(p, v) |\boldsymbol{f}(p) - \boldsymbol{f}(v)|^2 \ge 0$. The eigenvalues λ_ℓ of $\mathcal{L}$ are then nonnegative, associate with eigenvectors $\boldsymbol{u}_\ell : \mathcal{L}\, \boldsymbol{u}_\ell = \lambda_\ell\, \boldsymbol{u}_\ell,\ \ell = 1, \ldots, N$, and satisfying $0 = \lambda_1 \le \ldots \le \lambda_N$ with $\boldsymbol{u}_1 \equiv \frac{1}{\sqrt{N}}$. The set $\{(\boldsymbol{u}_\ell, \lambda_\ell)\}_{\ell=1}^N$ is then an orthonormal eigen-pair for $L_2(\mathcal{G})$. An orthonormal eigen-pair can be deduced from other positive semi-definite operators on $L_2(\mathcal{G})$, for example, diffusion operators.[19]

2.2 Tight frames and filter banks

Orthonormal bases are non-redundant systems for $L_2(\mathcal{G})$. This paper is concerned with construction of *redundant systems* for $L_2(\mathcal{G})$, which are frames with certain good properties for $L_2(\mathcal{G})$. Let $\{\boldsymbol{g}_\ell\}_{\ell=1}^M$ be a set of elements from $L_2(\mathcal{G})$. We say that $\{\boldsymbol{g}_\ell\}_{\ell=1}^M$ is a *frame* for $L_2(\mathcal{G})$ if there exist constants $0 < A \le B < \infty$, called *frame bounds*, such that

$$A\,\|\boldsymbol{f}\|^2 \le \sum_{\ell=1}^{M} |\langle \boldsymbol{f}, \boldsymbol{g}_\ell\rangle|^2 \le B\,\|\boldsymbol{f}\|^2 \quad \forall \boldsymbol{f} \in L_2(\mathcal{G}). \tag{3}$$

When $A = B = 1$, $\{\boldsymbol{g}_\ell\}_{\ell=1}^M$ is said to be a *tight frame* for $L_2(\mathcal{G})$, and by polarization identity, (3) is then equivalent to

$$\boldsymbol{f} = \sum_{\ell=1}^{M} \langle \boldsymbol{f}, \boldsymbol{g}_\ell\rangle\, \boldsymbol{g}_\ell. \tag{4}$$

When $\{\boldsymbol{g}_\ell\}_{\ell=1}^M$ is a tight frame and $\|\boldsymbol{g}_\ell\| = 1$ for $\ell = 1, \ldots, M$, we must have $M = N$ and $\{\boldsymbol{g}_\ell\}_{\ell=1}^N$ becomes an orthonormal basis for $L_2(\mathcal{G})$. Tight frames are of significance as we can use coefficients $\langle \boldsymbol{f}, \boldsymbol{g}_\ell\rangle$ to represent the vector $\boldsymbol{f}$.

A *filter* or *mask* $h := \{h_k\}_{k\in\mathbb{Z}} \subseteq \mathbb{C}$ is a complex-valued sequence in $l_1(\mathbb{Z}) := \{h = \{h_k\}_{k\in\mathbb{Z}} \subseteq \mathbb{C} : \sum_{k\in\mathbb{Z}} |h_k| < \infty\}$. A *filter bank* $\boldsymbol{\eta} = \{a; b^{(1)}, \ldots, b^{(r)}\}$ is a set of filters where a is usually a low-pass filter while others are high-pass filters. The *Fourier series* of a sequence $\{h_k\}_{k\in\mathbb{Z}}$ is defined to be the 1-periodic function $\widehat{h}(\xi) := \sum_{k\in\mathbb{Z}} h_k e^{-2\pi i k\xi}$, $\xi \in \mathbb{R}$.

Let $\Psi := \{\alpha; \beta^{(1)}, \ldots, \beta^{(r)}\}$ be a set of functions in $L_1(\mathbb{R})$, which is the space of absolutely integrable functions on $\mathbb{R}$ with respect to the Lebesgure measure. The *Fourier transform* $\widehat{\gamma}$ of a function $\gamma \in L_1(\mathbb{R})$ is defined to be $\widehat{\gamma}(\xi) := \int_{\mathbb{R}} \gamma(t) e^{-2\pi i t\xi}\,\mathrm{d}t$, $\xi \in \mathbb{R}$. The Fourier transform on $L_1(\mathbb{R})$ can be naturally extended to the space $L_2(\mathbb{R})$ of square integrable functions on $\mathbb{R}$. For $L_2(\mathbb{R})$, one can consider the (nonstationary nonhomogeneous) *affine system*

$$\mathsf{AS}_J(\{\Psi_j\}_{j=J}^{\infty}) = \{\alpha_j(2^J \cdot - k) : k \in \mathbb{Z}\} \cup \{\beta_j^{(n)}(2^j \cdot - k) : k \in \mathbb{Z}, n = 1, \ldots, r_j, j \ge J\}, \tag{5}$$

where $\Psi_j := \{\alpha_j; \beta_j^{(1)}, \ldots, \beta_j^{(r_j)}\} \subseteq L_2(\mathbb{R})$ are *framelet generators* at level j and two consecutive sets of framelet generators could be associated with a filter bank (see (7)). The sequences of affine systems have been extensively explored, such as for framelets on $\mathbb{R}^d$ and framelets on compact Riemannian manifolds.[20–24] Under certain extension principles such as the unitary extension principle (UEP),[25,26] the affine system $\mathsf{AS}_J(\{\Psi_j\}_{j=J}^{\infty})$ can be built to be a tight frame for $L_2(\mathbb{R})$. In such a case, the elements in the affine system $\mathsf{AS}_J(\{\Psi_j\}_{j=J}^{\infty})$ are called *tight framelets* for $L_2(\mathbb{R})$.

The purpose of this paper is to construct *tight framelets* for $L_2(\mathcal{G})$, which are based on affine systems on $\mathbb{R}$. We next introduce one of such tight framelets on $L_2(\mathcal{G})$, call *decimated tight framelets* on $\mathcal{G}$.

2.3 Decimated tight framelets on $\mathcal{G}$

Let $\mathcal{G} = (V, E, \boldsymbol{w})$ be a graph and $\mathcal{G}_{J\to J_0} := (\mathcal{G}_J, \ldots, \mathcal{G}_{J_0})$ be a coarse-grained chain of $\mathcal{G}$. For each vertex $[p]$ in $\mathcal{G}_j = (V_j, E_j, \boldsymbol{w}_j)$, we assign a real number $\omega_{j,[p]} \in \mathbb{R}$, called the *(associated) weight*. For the bottom level when $j = J$, we let $\omega_{J,[p]_{\mathcal{G}_J}} \equiv 1$ for all $[p]_{\mathcal{G}_J} = \{p\}$ in V_J. Let $\mathcal{Q}_j := \{\omega_{j,[p]} : [p] \in V_j\}$ be the set of weights on $\mathcal{G}_j$ and $\mathcal{Q}_{J\to J_0} := (\mathcal{Q}_J, \ldots, \mathcal{Q}_{J_0})$ be the sequence of weights for the coarse-grained chain $\mathcal{G}_{J\to J_0}$.

Let $\{(\boldsymbol{u}_\ell, \lambda_\ell)\}_{\ell=1}^N$ be an orthonormal eigen-pair for $L_2(\mathcal{G})$. For $\mathcal{Q}_j = \{\omega_{j,[p]} : [p] \in V_j\}$ on $\mathcal{G}_j$, we define

$$\mathcal{U}_{\ell,\ell'}(\mathcal{Q}_j) := \sum_{[p]\in V_j} \omega_{j,[p]}\, \boldsymbol{u}_\ell([p])\overline{\boldsymbol{u}_{\ell'}([p])}. \tag{6}$$

Note that $\mathcal{U}_{\ell,\ell'}(\mathcal{Q}_J) = \delta_{\ell,\ell'}$ since $\omega_{J,[p]} \equiv 1$ and $[p]_{\mathcal{G}_J} = \{p\}$ is a singleton.

Let $\Psi_j = \{\alpha_j; \beta_j^{(1)}, \ldots, \beta_j^{(r_j)}\}$ be a set of functions in $L_1(\mathbb{R})$ at level j for $j = J_0, \ldots, J$. Ψ_j and Ψ_{j-1} are connected by a filter bank $\boldsymbol{\eta}_j := \{a_j; b_j^{(1)}, \ldots, b_j^{(r_{j-1})}\}$ in that, for $\xi \in \mathbb{R}$ and $0 < \Lambda_{J_0} \le \Lambda_{J_0+1} \le \cdots \le \Lambda_J < \infty$,

$$\begin{aligned}
\widehat{\alpha_{j-1}}(\xi/\Lambda_{j-1}) &= \widehat{a_j}(\xi/\Lambda_j)\widehat{\alpha_j}(\xi/\Lambda_j),\\
\widehat{\beta_{j-1}^{(n)}}(\xi/\Lambda_{j-1}) &= \widehat{b_j^{(n)}}(\xi/\Lambda_j)\widehat{\alpha_j}(\xi/\Lambda_j), \quad n = 1, \ldots, r_{j-1}.
\end{aligned} \tag{7}$$

Typical example of $\Lambda_j = 2^j$. The *decimated framelets* $\boldsymbol{\varphi}_{j,[p]}(v)$ and $\boldsymbol{\psi}_{j,[p]}^{(n)}(v)$, $p, v \in V$, at level $j = J_0, \ldots, J$ for the coarse-grained chain $\mathcal{G}_{J\to J_0}$ of the graph $\mathcal{G}$ and framelet generators in (7) are

$$\begin{aligned}
\boldsymbol{\varphi}_{j,[p]}(v) &:= \sqrt{\omega_{j,[p]}} \sum_{\ell=1}^{N} \widehat{\alpha_j}\left(\frac{\lambda_\ell}{\Lambda_j}\right) \overline{\boldsymbol{u}_\ell([p])} \boldsymbol{u}_\ell(v), \quad [p] \in V_j,\\
\boldsymbol{\psi}_{j,[p]}^{(n)}(v) &:= \sqrt{\omega_{j+1,[p]}} \sum_{\ell=1}^{N} \widehat{\beta_j^{(n)}}\left(\frac{\lambda_\ell}{\Lambda_j}\right) \overline{\boldsymbol{u}_\ell([p])} \boldsymbol{u}_\ell(v), \quad [p] \in V_{j+1},\ n = 1, \ldots, r_j,
\end{aligned} \tag{8}$$

where for $j = J$, we let $V_{J+1} := V_J$ and $\omega_{J+1,[p]} := \omega_{J,[p]}$, and $\boldsymbol{u}_\ell([p])$ can be defined by $\boldsymbol{u}_\ell([p]) := \min_{v\in[p]} \boldsymbol{u}_\ell(v)$.

The *(decimated) framelet system* $\mathsf{DFS}(\{\Psi_j\}_{j=J_1}^J, \{\boldsymbol{\eta}_j\}_{j=J_1+1}^J)$ on $\mathcal{G}$ (starting at level J_1) is a (nonhomogeneous nonstationary) affine system given by

$$\begin{aligned}
\mathsf{DFS}(\{\Psi_j\}_{j=J_1}^J, \{\boldsymbol{\eta}_j\}_{j=J_1+1}^J) &:= \mathsf{DFS}(\{\Psi_j\}_{j=J_1}^J, \{\boldsymbol{\eta}_j\}_{j=J_1+1}^J; \mathcal{G}_{J\to J_1}, \mathcal{Q}_{J\to J_1})\\
&:= \{\boldsymbol{\varphi}_{J_1,[p]} : [p] \in V_{J_1}\} \cup \{\boldsymbol{\psi}_{j,[p]}^{(n)} : [p] \in V_{j+1},\ j = J_1, \ldots, J\}.
\end{aligned} \tag{9}$$

The following theorem gives equivalence conditions of the tightness of a sequence of decimated framelet systems for a coarse-grained chain of a graph.

THEOREM 2.1. *Let $\Psi_j := \{\alpha_j; \beta_j^{(1)}, \ldots, \beta_j^{(r_j)}\}$, $j = J_0, \ldots, J$ be a sequence of framelet generators sets in $L_1(\mathbb{R})$ associated with a sequence of filter banks $\boldsymbol{\eta}_j = \{a_j; b_j^{(1)}, \ldots, b_j^{(r_{j-1})}\}$, $j = J_0+1, \ldots, J$, see (7). Let $\mathcal{G}_{J\to J_0}$ be a coarse-grained chain of a graph $\mathcal{G}$ with a weight sequence $\mathcal{Q}_{J\to J_0}$. Let $\mathsf{DFS}(\{\Psi_j\}_{j=J_1}^J, \{\boldsymbol{\eta}_j\}_{j=J_1+1}^J)$, $J_1 = J_0, \ldots, J$ be a sequence of decimated framelet systems for the coarse-grained chain $\mathcal{G}_{J\to J_0}$ with framelets in (8). Then, the following statements are equivalent.*

(i) *The decimated framelet system $\mathsf{DFS}(\{\Psi_j\}_{j=J_1}^J, \{\boldsymbol{\eta}_j\}_{j=J_1+1}^J)$ is a tight frame for $L_2(\mathcal{G})$ for all $J_1 = J_0, \ldots, J$, that is, for all $J_1 = J_0, \ldots, J$,*

$$\|\boldsymbol{f}\|^2 = \sum_{[p]\in V_{J_1}} \left|\left\langle \boldsymbol{f}, \boldsymbol{\varphi}_{J_1,[p]} \right\rangle\right|^2 + \sum_{j=J_1}^{J} \sum_{n=1}^{r_j} \sum_{[p]\in V_{j+1}} \left|\left\langle \boldsymbol{f}, \boldsymbol{\psi}_{j,[p]}^{(n)} \right\rangle\right|^2 \quad \forall \boldsymbol{f} \in L_2(\mathcal{G}). \tag{10}$$

(ii) *The framelet generators in Ψ_j and the weights in $\mathcal{Q}_j$ satisfy*

$$1 = \left|\widehat{\alpha_j}\left(\frac{\lambda_\ell}{\Lambda_J}\right)\right|^2 + \sum_{n=1}^{r_J} \left|\widehat{\beta_j^{(n)}}\left(\frac{\lambda_\ell}{\Lambda_J}\right)\right|^2, \quad \ell = 1, \ldots, N, \tag{11}$$

$$\begin{aligned}
&\overline{\widehat{\alpha_{j+1}}\left(\frac{\lambda_\ell}{\Lambda_{j+1}}\right)} \widehat{\alpha_{j+1}}\left(\frac{\lambda_{\ell'}}{\Lambda_{j+1}}\right) \mathcal{U}_{\ell,\ell'}(\mathcal{Q}_{j+1}) - \overline{\widehat{\alpha_j}\left(\frac{\lambda_\ell}{\Lambda_j}\right)} \widehat{\alpha_j}\left(\frac{\lambda_{\ell'}}{\Lambda_j}\right) \mathcal{U}_{\ell,\ell'}(\mathcal{Q}_j)\\
&\quad = \sum_{n=1}^{r_j} \overline{\widehat{\beta_j^{(n)}}\left(\frac{\lambda_\ell}{\Lambda_j}\right)} \widehat{\beta_j^{(n)}}\left(\frac{\lambda_{\ell'}}{\Lambda_j}\right) \mathcal{U}_{\ell,\ell'}(\mathcal{Q}_{j+1}),
\end{aligned} \tag{12}$$

for all $1 \le \ell, \ell' \le N$ and $j = J_0, \ldots, J-1$, where $\mathcal{U}_{\ell,\ell'}(\mathcal{Q}_j)$ is given by (6).

(iii) *The identities in* (11) *hold and*

$$\overline{\widehat{a_j}\left(\frac{\lambda_\ell}{\Lambda_j}\right)}\widehat{a_j}\left(\frac{\lambda_{\ell'}}{\Lambda_j}\right)\mathcal{U}_{\ell,\ell'}(\mathcal{Q}_{j-1})+\sum_{n=1}^{r_{j-1}}\overline{\widehat{b_j^{(n)}}\left(\frac{\lambda_\ell}{\Lambda_j}\right)}\widehat{b_j^{(n)}}\left(\frac{\lambda_{\ell'}}{\Lambda_j}\right)\mathcal{U}_{\ell,\ell'}(\mathcal{Q}_j)=\mathcal{U}_{\ell,\ell'}(\mathcal{Q}_j), \tag{13}$$

for all $(\ell,\ell')\in\sigma^{(j)}_{\alpha,\overline{\alpha}}$ *and for all* $j=J_0+1,\dots,J$, *where*

$$\sigma^{(j)}_{\alpha,\overline{\alpha}}:=\left\{(\ell,\ell')\in\mathbb{N}\times\mathbb{N}:\ \overline{\widehat{\alpha}\left(\frac{\lambda_\ell}{\Lambda_j}\right)}\widehat{\alpha}\left(\frac{\lambda_{\ell'}}{\Lambda_j}\right)\neq 0\right\}. \tag{14}$$

In particular, if

$$\sigma^{(j)}_{\alpha,\overline{\alpha}}\subseteq\sigma^{(j+1)}_{\alpha,\overline{\alpha}}\quad\textit{and}\quad\mathcal{U}_{\ell,\ell'}(\mathcal{Q}_j)=\delta_{\ell,\ell'}\quad\forall(\ell,\ell')\in\sigma^{(j)}_{\alpha,\overline{\alpha}},\ j=J_0,\dots,J-1. \tag{15}$$

then (12) *is reduced to*

$$\left|\widehat{\alpha_{j+1}}\left(\frac{\lambda_\ell}{\Lambda_{j+1}}\right)\right|^2=\left|\widehat{\alpha_j}\left(\frac{\lambda_\ell}{\Lambda_j}\right)\right|^2+\sum_{n=1}^{r_j}\left|\widehat{\beta_j^{(n)}}\left(\frac{\lambda_\ell}{\Lambda_j}\right)\right|^2 \tag{16}$$

for $j=J_0,\dots,J-1$ *and* $\ell=1,\dots,N$, *and* (13) *is reduced to*

$$\left|\widehat{a_j}\left(\frac{\lambda_\ell}{\Lambda_j}\right)\right|^2+\sum_{n=1}^{r_{j-1}}\left|\widehat{b_j^{(n)}}\left(\frac{\lambda_\ell}{\Lambda_j}\right)\right|^2=1, \tag{17}$$

for $j=J_0+1,\dots,J$ *and* $\ell=1,\dots,N$.

3. FAST DISCRETE FRAMELET TRANSFORMS ON $\mathcal{G}$

Given a vector of data $\boldsymbol{f}$ defined on a graph $\mathcal{G}$ and a sequence of decimated tight framelets as in (9), the *framelet decomposition* algorithm produces a sequence of the vectors of the framelet approximation and detail coefficients

$$\{\mathbf{v}_{J_0}\}\cup\{\mathbf{w}_j^{(n)}:n=1,\dots,r_j,\ j=J_0,\dots,J\} \tag{18}$$

where for level $j=J_0,\dots,J$, $\mathbf{v}_j$ is the vector of the approximation framelet coefficients on $\mathcal{G}_j$ and $\mathbf{w}_j^{(n)}$, $n=1,\dots,r_j$, are the vector of the detail framelet coefficients on $\mathcal{G}_{j+1}$ given as follows:

$$\begin{aligned}\mathbf{v}_j([p])&:=\left\langle f,\boldsymbol{\varphi}_{j,[p]}\right\rangle,\quad [p]\in V_j,\\ \mathbf{w}_j^{(n)}([p])&:=\left\langle f,\boldsymbol{\psi}^{(n)}_{j,[p]}\right\rangle,\quad [p]\in V_{j+1},\ n=1,\dots,r_j.\end{aligned} \tag{19}$$

The *framelet reconstruction* algorithm is to reconstruct $\boldsymbol{f}$ with the framelet coefficients in (18). As follows, we investigate the constructive implementation of the framelet reconstruction.

Let $\{(\boldsymbol{u}_\ell,\lambda_\ell)\}_{\ell=1}^N$ be an orthonormal eigen-pair for $L_2(\mathcal{G})$. For $j=J_0,\dots,J$, let $\mathcal{Q}_j:=\{\omega_{j,[p]}:[p]\in V_j\}$ be the set of weights on $\mathcal{G}_j$ and $\mathcal{Q}_{J\to J_0}:=(\mathcal{Q}_J,\dots,\mathcal{Q}_{J_0})$ for the coarse-grained chain $\mathcal{G}_{J\to J_0}$ which satisfies (15). For a finite index set Ω, we denote by $l(\Omega):=\{\boldsymbol{c}:\Omega\to\mathbb{C}\}$ all sequences supported on Ω. For $j=J_0,\dots,J$, let $\Omega_j:=\{\ell:1\le\ell\le N_j\}$, where $N_j:=|V_j|$, and $l(\Omega_j)$ and $l(V_j)$ the sequences supported on Ω_j and V_j respectively.

Define $\mathbf{F}_j:l(\Lambda_j)\to l(V_j)$ the *discrete Fourier transform* (DFT) operator on $\mathcal{G}_j$ as

$$[\mathbf{F}_j\boldsymbol{c}]([p]):=\sum_{\ell\in\Omega_j}c_\ell\sqrt{\omega_{j,[p]}}\,\boldsymbol{u}_\ell([p]),\quad [p]\in V_j,\ \boldsymbol{c}=(c_\ell)_{\ell=1}^{N_j}\in l(\Omega_j). \tag{20}$$

We say the sequence $(\mathbf{F}_j\boldsymbol{c})$ a (Ω_j,V_j)-*sequence* and $\widehat{\mathbf{F}_j\boldsymbol{c}}:=\boldsymbol{c}$ the sequence of *discrete Fourier coefficients* of $\mathbf{F}_j\boldsymbol{c}$. Let $l(\Omega_j,V_j)$ be the set of all (Ω_j,V_j)-sequences.

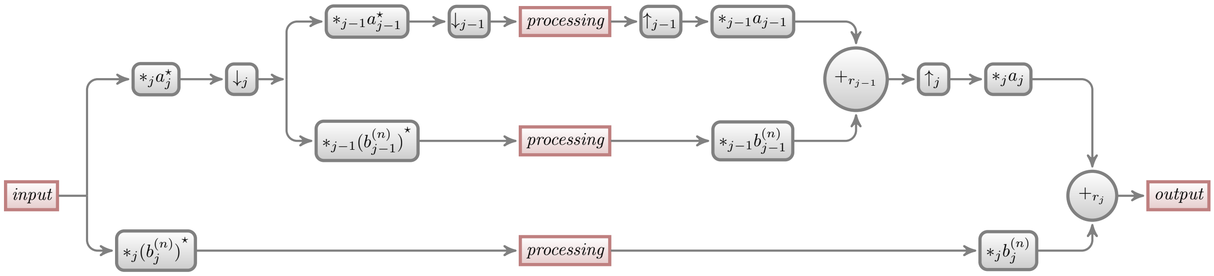

Figure 1: Two-level $\mathcal{G}$-framelet decomposition and reconstruction based on the filter banks $\{a_{j-1}; b_{j-1}^{(1)}, \dots, b_{j-1}^{(r_{j-1})}\}$ and $\{a_j; b_j^{(1)}, \dots, b_j^{(r_j)}\}$.

The *adjoint discrete Fourier transform* (ADFT) $\mathbf{F}_j^* : l(V_j) \to l(\Omega_j)$ on $\mathcal{G}_j$ is

$$(\mathbf{F}_j^* \mathbf{v})_\ell := \sum_{[p] \in V_j} \mathbf{v}([p]) \sqrt{\omega_{j,[p]}}\, \overline{\boldsymbol{u}_\ell([p])}, \quad \ell \in \Omega_j. \tag{21}$$

We say the sequence $\mathbf{F}_j^* \mathbf{v}$ a (V_j, Ω_j)-*sequence* and let $l(V_j, \Omega_j)$ be the set of all (V_j, Ω_j)-sequences.

Proposition 1. *Let $\{(\boldsymbol{u}_\ell, \lambda_\ell)\}_{\ell=1}^N$ be an orthonormal eigen-pair for $L_2(\mathcal{G})$. Let $\mathcal{Q}_{J \to J_0}$ be a weight sequence for $\mathcal{G}_{J \to J_0}$ which satisfies (15). Let $\mathbf{F}_j$ and $\mathbf{F}_j^*$ be the DFT and ADFT for $\{(\boldsymbol{u}_\ell, \lambda_\ell)\}_{\ell=1}^N$ given in (20) and (21). Then, $\mathbf{F}_j$ and $\mathbf{F}_j^*$ satisfy*

$$\mathbf{F}_j^* \mathbf{F}_j = \mathbf{I}_{V_j} \quad \textit{and} \quad \mathbf{F}_j \mathbf{F}_j^* = \mathbf{I}_{\Omega_j},$$

where $\mathbf{I}_{V_j}$ and $\mathbf{I}_{\Omega_j}$ are the identity operators on $l(V_j)$ and $l(\Omega_j)$, respectively.

Consequently, for every (Ω_j, V_j)-sequence $\mathbf{v}$, there exists a *unique* sequence $\boldsymbol{c} \in l(\Omega_j)$ such that $\mathbf{F}_j \boldsymbol{c} = \mathbf{v}$. Hence, the discrete Fourier coefficients $\widehat{\mathbf{v}} := \boldsymbol{c} = \mathbf{F}_j^* \mathbf{v}_j$ of $\mathbf{v}$ are well-defined.

Based on the discrete Fourier transform operators, we next define convolution, downsampling, and upsampling operators.

Let $h \in l_1(\mathbb{Z})$ be a filter and $\mathbf{v} \in l(\Omega_j, V_j)$ be a (Ω_j, V_j)-sequence. Let $\widehat{\mathbf{v}} := (\widehat{\mathrm{v}}_\ell)_{\ell \in \Omega_j}$ be its discrete Fourier coefficient sequence. The *discrete convolution* $\mathbf{v} *_j h$ is defined as the following sequence in $l(\Omega_j, V_j)$:

$$[\mathbf{v} *_j h]([p]) := \sum_{\ell \in \Omega_j} \widehat{\mathrm{v}}_\ell\, \widehat{h}\left(\frac{\lambda_\ell}{\lambda_{N_j}}\right) \sqrt{\omega_{j,[p]}}\, \boldsymbol{u}_\ell([p]), \quad [p] \in V_j. \tag{22}$$

That is, $(\widehat{\mathbf{v} *_j h})_\ell = \widehat{\mathrm{v}}_\ell\, \widehat{h}\left(\frac{\lambda_\ell}{2^j}\right)$ for $\ell \in \Omega_j$. We define the *downsampling operator* $\downarrow_j$: $l(\Omega_j, V_j) \to l(\Omega_{j-1}, V_{j-1})$ for a (Ω_j, V_j)-sequence $\mathbf{v}$ by

$$[\mathbf{v}\downarrow_j]([p]) := \sum_{\ell \in \Omega_{j-1}} \widehat{\mathrm{v}}_\ell \sqrt{\omega_{j-1,[p]}}\, \boldsymbol{u}_\ell([p]), \quad [p] \in V_{j-1}. \tag{23}$$

The *upsampling operator* $\uparrow_j$: $l(\Omega_{j-1}, V_{j-1}) \to l(\Omega_j, V_j)$ for a sequence $\mathbf{v} \in l(\Omega_{j-1}, V_{j-1})$ is defined by

$$[\mathbf{v}\uparrow_j]([p]) := \sum_{\ell \in \Omega_{j-1}} \widehat{\mathrm{v}}_\ell \sqrt{\omega_{j,[p]}}\, \boldsymbol{u}_\ell([p]), \quad [p] \in V_j. \tag{24}$$

For a filter $h \in l_1(\mathbb{Z})$, we denote $h^\star$ a filter such that $\widehat{h^\star}(\xi) = \overline{\widehat{h}(\xi)}$, $\xi \in \mathbb{R}$. For a sequence of data $\mathbf{v}_{J_1} \in l(\Lambda_{J_1}, \Omega_{J_1})$, $J_0 \le J_1 \le J$ on $\mathcal{G}$, the *multi-level framelet decomposition on $\mathcal{G}$* is

$$\mathbf{v}_{j-1} = (\mathbf{v}_j *_j a_j^\star)\downarrow_j, \quad \mathbf{w}_{j-1}^{(n)} = (\mathbf{v}_j *_j (b_j^{(n)})^\star), \quad n = 1, \dots, r_{j-1},\ j = J, \dots, J_1 + 1.$$

For a sequence $(\mathbf{w}_{J-1}^{(1)}, \ldots, \mathbf{w}_{J-1}^{(r_{J-1})}, \ldots, \mathbf{w}_{J_0}^{(1)}, \ldots, \mathbf{w}_{J_0}^{(r_{J_0})}, \mathbf{v}_{J_0})$ of the framelet coefficients derived from a multi-level decomposition, the *multi-level $\mathcal{G}$-framelet reconstruction* is

$$\mathbf{v}_j = (\mathbf{v}_{j-1}{\uparrow}_j) *_j a_j + \sum_{n=1}^{r_{j-1}} \mathbf{w}_{j-1}^{(n)} *_j b_j^{(n)}, \ j = J_0+1, \ldots, J.$$

Figure 1 illustrates the flowchart for the two-level decomposition and reconstruction $\mathcal{G}$-framelet transforms.

4. A TOY EXAMPLE TO ILLUSTRATE CONSTRUNCTIONS

In this section, we show the full steps of the constructions of the decimated framelet system on a graph using the following toy example. Consider a graph $\mathcal{G} = (V, E, \boldsymbol{w})$ determined by

$$V := \{a, b, c, d, e, f\} \text{ and } E = \{(a,b), (a,c), (c,d), (c,e), (c,f), (d,e)\}.$$

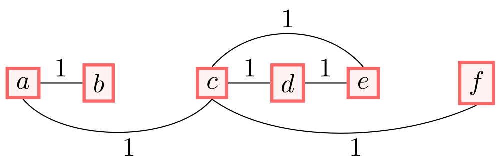

Figure 2: Graph $\mathcal{G}$, where the vertices are represented by the boxes and the edges are by the lines for the pairs of connected vertices, and the weight for each edge is 1.

We apply the NHC clustering algorithm[18] to the graph $\mathcal{G} =: \mathcal{G}_3$ which is at the bottom level 3 with three initial centers $\{a\}, \{c\}, \{f\}$ to cluster $\mathcal{G}_3$ to $\mathcal{G}_2$ at level 2, which has 3 clusters, and next cluster $\mathcal{G}_2$ to $\mathcal{G}_1$ at level 1 with 2 clusters, and eventually to $\mathcal{G}_0$ with 1 cluster at the root. See Figure 3 for the resulting coarse-grained chain of $\mathcal{G}$. The details of the coarse-grained chain $\mathcal{G}_{3\to 0} = (\mathcal{G}_3, \mathcal{G}_2, \mathcal{G}_1, \mathcal{G}_0)$ are as follow.

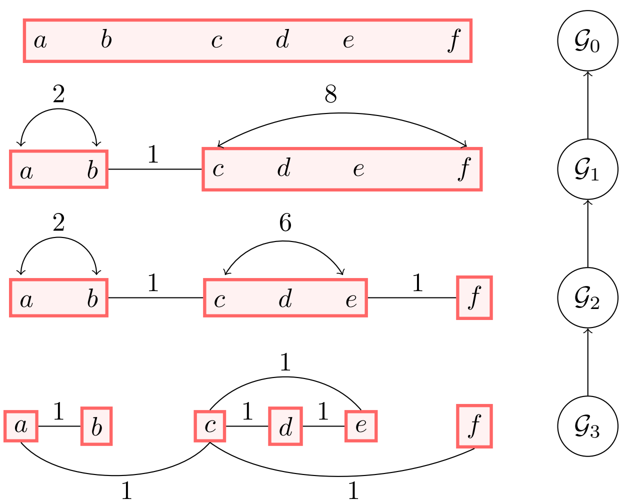

Figure 3: Coarse-grained chain of $\mathcal{G}$. Here the arc on a same cluster indicates a self-loop.

(1) At level 3, $\mathcal{G}_3 := \mathcal{G}$, of which each vertex is a leaf and a cluster of singleton. The graph $\mathcal{G}$ is associated with the adjacency matrix $\boldsymbol{w}$, the degree matrix $\boldsymbol{d}$, and the graph Laplacian matrix $\boldsymbol{\mathcal{L}} := \boldsymbol{d} - \boldsymbol{w}$:

$$\boldsymbol{w} = \begin{bmatrix} 0 & 1 & 1 & 0 & 0 & 0 \\ 1 & 0 & 0 & 0 & 0 & 0 \\ 1 & 0 & 0 & 1 & 1 & 1 \\ 0 & 0 & 1 & 0 & 1 & 0 \\ 0 & 0 & 1 & 1 & 0 & 0 \\ 0 & 0 & 1 & 0 & 0 & 0 \end{bmatrix}, \ \boldsymbol{d} = \begin{bmatrix} 2 & 0 & 0 & 0 & 0 & 0 \\ 0 & 1 & 0 & 0 & 0 & 0 \\ 0 & 0 & 4 & 0 & 0 & 0 \\ 0 & 0 & 0 & 2 & 0 & 0 \\ 0 & 0 & 0 & 0 & 2 & 0 \\ 0 & 0 & 0 & 0 & 0 & 1 \end{bmatrix}, \ \boldsymbol{\mathcal{L}} = \begin{bmatrix} 2 & -1 & -1 & 0 & 0 & 0 \\ -1 & 1 & 0 & 0 & 0 & 0 \\ -1 & 0 & 4 & -1 & -1 & -1 \\ 0 & 0 & -1 & 2 & -1 & 0 \\ 0 & 0 & -1 & -1 & 2 & 0 \\ 0 & 0 & -1 & 0 & 0 & 1 \end{bmatrix}, \quad (25)$$

where the row or column is with respect to the vertices ordered as a, b, c, d, e, f.

(2) At level 2, we obtain three clusters $[a]_{\mathcal{G}_2} = \{a, b\}$, $[c]_{\mathcal{G}_2} = \{c, d, e\}$, and $[f]_{\mathcal{G}_2} = \{f\}$ for the coarse-grained graph $\mathcal{G}_2 := (V_2, E_2, \boldsymbol{w}_2)$ of $\mathcal{G}_3$, where $V_2 = \{[a]_{\mathcal{G}_2}, [c]_{\mathcal{G}_2}, [f]_{\mathcal{G}_2}\}$, $E_2 = \{([a]_{\mathcal{G}_2}, [a]_{\mathcal{G}_2}), ([a]_{\mathcal{G}_2}, [c]_{\mathcal{G}_2}), ([c]_{\mathcal{G}_2}, [c]_{\mathcal{G}_2}), ([c]_{\mathcal{G}_2}, [f]_{\mathcal{G}_2})\}$, and

$$\boldsymbol{w}_2 = \frac{1}{12}\begin{bmatrix} 2 & 1 & 0 \\ 1 & 6 & 1 \\ 0 & 1 & 0 \end{bmatrix}, \ \boldsymbol{d}_2 = \frac{1}{12}\begin{bmatrix} 3 & 0 & 0 \\ 0 & 8 & 0 \\ 0 & 0 & 1 \end{bmatrix}, \ \mathcal{L}_2 = \frac{1}{12}\begin{bmatrix} 1 & -1 & 0 \\ -1 & 2 & -1 \\ 0 & -1 & 1 \end{bmatrix}. \tag{26}$$

(3) At level 1, we obtain two clusters $[a]_{\mathcal{G}_1} = \{a, b\}$ and $[c]_{\mathcal{G}_1} = \{c, d, e, f\}$ for the coarse-grained graph $\mathcal{G}_1 := (V_1, E_1, \boldsymbol{w}_1)$ of $\mathcal{G}_2$, where $V_1 = \big\{[a]_{\mathcal{G}_1}, [c]_{\mathcal{G}_1}\big\}$, $E_1 = \big\{([a]_{\mathcal{G}_1}, [a]_{\mathcal{G}_1}), ([a]_{\mathcal{G}_1}, [c]_{\mathcal{G}_1}), ([c]_{\mathcal{G}_1}, [c]_{\mathcal{G}_1})\big\}$, and

$$\boldsymbol{w}_1 = \frac{1}{12}\begin{bmatrix} 2 & 1 \\ 1 & 8 \end{bmatrix}, \ \boldsymbol{d}_2 = \frac{1}{12}\begin{bmatrix} 3 & 0 \\ 0 & 9 \end{bmatrix}, \ \mathcal{L}_1 = \frac{1}{12}\begin{bmatrix} 1 & -1 \\ -1 & 1 \end{bmatrix}. \tag{27}$$

(4) At level 0, we reach the root $\mathcal{G}_0 := (V_0, E_0, \boldsymbol{w}_0)$, where $V_0 = \{[a, b, c, d, e, f] =: [a]_{\mathcal{G}_0}\}$ has only one cluster $[a]_{\mathcal{G}_0}$ which contains all vertices from $\mathcal{G}$, $E_0 = \{([a]_{\mathcal{G}_0}, [a]_{\mathcal{G}_0})\}$, and $\boldsymbol{w}_0 = \frac{1}{12}$.

Next, we build an orthonormal eigen-pair $\{(\boldsymbol{u}_\ell, \lambda_\ell)\}_{\ell=1}^{6}$ for $L_2(\mathcal{G})$ using information of the coarse-grained chain $\mathcal{G}_{3\to 0}$ from level 0 to level 3 so that it satisfies for $j = 0, 1, 2, 3$

$$\boldsymbol{u}_\ell(v) \equiv const \quad \forall v \in [v]_{\mathcal{G}_j} \text{ and } \forall \ell \le |V_j|. \tag{28}$$

(5) At level 0, $\mathcal{G}_0$ is a graph of singleton. In this case, $\lambda_1^{\mathcal{G}_0} = 0$ and $\boldsymbol{u}_1^{\mathcal{G}_0} = 1$. Simply set

$$\boldsymbol{u}_1 = \frac{1}{\sqrt{6}}\begin{bmatrix} 1 & 1 & 1 & 1 & 1 & 1 \end{bmatrix}^\top.$$

(6) At level 1, the eigenvalues of $\mathcal{L}_1$ as in (27) are $\lambda_1^{\mathcal{G}_1} = 0$ and $\lambda_2^{\mathcal{G}_1} = \frac{2}{12}$. The eigenvectors of $\mathcal{L}_1$ with respect to 0, $\frac{2}{12}$ are

$$\boldsymbol{u}_1^{\mathcal{G}_1} = \frac{1}{\sqrt{2}}\begin{bmatrix} 1 & 1 \end{bmatrix}^\top, \quad \boldsymbol{u}_2^{\mathcal{G}_1} = \frac{1}{\sqrt{2}}\begin{bmatrix} 1 & -1 \end{bmatrix}^\top.$$

We extend $\boldsymbol{u}_2^{\mathcal{G}_1}$, with respect to clusters $[a]_{\mathcal{G}_1}$ and $[c]_{\mathcal{G}_1}$, to $\boldsymbol{u}_2^{(1)}$ on $\mathcal{G}$ as

$$\boldsymbol{u}_2^{(1)} = \frac{1}{\sqrt{6}}\begin{bmatrix} 1 & 1 & -1 & -1 & -1 & -1 \end{bmatrix}^\top.$$

Apply the Gram-Schmidt orthonormalization process to $\{\boldsymbol{u}_1, \boldsymbol{u}_2^{(1)}\}$, we then obtain a new vector $\boldsymbol{u}_2$:

$$\boldsymbol{u}_2 = \frac{1}{4\sqrt{3}}\begin{bmatrix} 4 & 4 & -2 & -2 & -2 & -2 \end{bmatrix}^\top.$$

(7) At level 2, the eigenvalues of $\mathcal{L}_2$ in (26) are $\lambda_1^{\mathcal{G}_2} = 0$, $\lambda_2^{\mathcal{G}_2} = \frac{1}{12}$, $\lambda_3^{\mathcal{G}_2} = \frac{3}{12}$. The eigenvectors of $\mathcal{L}_2$ with respect to 0, $\frac{1}{12}$, $\frac{3}{12}$ are

$$\boldsymbol{u}_1^{\mathcal{G}_2} = \frac{1}{\sqrt{3}}\begin{bmatrix} 1 & 1 & 1 \end{bmatrix}^\top, \quad \boldsymbol{u}_2^{\mathcal{G}_2} = \frac{1}{\sqrt{2}}\begin{bmatrix} 1 & 0 & -1 \end{bmatrix}^\top, \quad \boldsymbol{u}_3^{\mathcal{G}_2} = \frac{1}{\sqrt{6}}\begin{bmatrix} 1 & -2 & 1 \end{bmatrix}^\top.$$

We extend $\boldsymbol{u}_3^{\mathcal{G}_2}$, with respect to clusters $[a]_{\mathcal{G}_2}$, $[c]_{\mathcal{G}_2}$ and $[f]_{\mathcal{G}_2}$, to $\boldsymbol{u}_3^{(2)}$ on $\mathcal{G}$ as

$$\boldsymbol{u}_3^{(2)} = \frac{1}{\sqrt{6}}\begin{bmatrix} 1 & 1 & -1 & -1 & -1 & 1 \end{bmatrix}^\top.$$

Apply the Gram-Schmidt orthonormalization process to $\{\boldsymbol{u}_1, \boldsymbol{u}_2, \boldsymbol{u}_3^{\mathcal{G}_3}\}$, we then obtain a new vector $\boldsymbol{u}_3$:

$$\boldsymbol{u}_3 = \frac{1}{4\sqrt{3}}\begin{bmatrix} 0 & 0 & -2 & -2 & -2 & 6 \end{bmatrix}^\top.$$

(8) Continue the above similar steps, at level 3, from the graph Laplacian in (25), we obtain an orthonormal basis $\{\boldsymbol{u}_1, \ldots, \boldsymbol{u}_6\}$ for $L_2(\mathcal{G})$ satisfying (28) as

$$
\begin{aligned}
\boldsymbol{u}_1 &= \frac{1}{\sqrt{6}}\begin{bmatrix}1 & 1 & 1 & 1 & 1 & 1\end{bmatrix}^\top,\\
\boldsymbol{u}_2 &= \frac{1}{4\sqrt{3}}\begin{bmatrix}4 & 4 & -2 & -2 & -2 & -2]\end{bmatrix}^\top,\\
\boldsymbol{u}_3 &= \frac{1}{4\sqrt{3}}\begin{bmatrix}0 & 0 & -2 & -2 & -2 & 6\end{bmatrix}^\top,\\
\boldsymbol{u}_4 &= \frac{1}{\sqrt{6}}\begin{bmatrix}0 & 0 & 2 & -1 & -1 & 0\end{bmatrix}^\top,\\
\boldsymbol{u}_5 &= \frac{1}{\sqrt{2}}\begin{bmatrix}0 & 0 & 0 & 1 & -1 & 0\end{bmatrix}^\top,\\
\boldsymbol{u}_6 &= \frac{1}{\sqrt{2}}\begin{bmatrix}1 & -1 & 0 & 0 & 0 & 0\end{bmatrix}^\top.
\end{aligned}
$$

We set $\lambda_\ell = \ell - 1$ for $\ell = 1, \ldots, 6$.

Based on the orthonormal eigen-pair $\{(\boldsymbol{u}_\ell, \lambda_\ell)\}_{\ell=1}^{6}$, we next construct decimated framelet systems as in (9).

(9) At level 3, $\mathcal{G}_3 \equiv \mathcal{G}$ and $[p]_{\mathcal{G}_3} = \{p\} \in V_3$ are singletons. Simply set $\omega_{j,[p]} = 1$ for all $p \in V$. Setting $\widehat{\alpha_3}\left(\frac{\lambda_\ell}{\Lambda_3}\right) \equiv 1$ for all ℓ, by (8), we get

$$
\boldsymbol{\varphi}_{3,[p]}(v) = \boldsymbol{\varphi}_{3,p} = \delta_{[p],v}, \quad p, v \in V.
$$

No framelets $\boldsymbol{\psi}_{j,[p]}^{(n)}(v)$ at this level. The system $\{\boldsymbol{\varphi}_{3,[p]} : [p] \in V_3\} = \{\delta_{p,v} : p, v \in V\}$ is the trivial orthonormal basis.

(10) At level 2, set

$$
\widehat{\alpha_2}\left(\frac{\lambda_\ell}{\Lambda_2}\right) = \begin{cases} 1 & \ell = 1,2; \\ \frac{1}{\sqrt{2}} & \ell = 3; \\ 0 & \text{otherwise.} \end{cases} \quad \widehat{\beta_2^{(1)}}\left(\frac{\lambda_\ell}{\Lambda_2}\right) = \begin{cases} \frac{1}{\sqrt{2}} & \ell = 3,5; \\ 1 & \ell = 4; \\ 0 & \text{otherwise.} \end{cases} \quad \widehat{\beta_2^{(2)}}\left(\frac{\lambda_\ell}{\Lambda_2}\right) = \begin{cases} \frac{1}{\sqrt{2}} & \ell = 5; \\ 1 & \ell = 6; \\ 0 & \text{otherwise.} \end{cases}
$$

Note that $|\widehat{\alpha_2}|^2 + |\widehat{\beta_2^{(1)}}|^2 + |\widehat{\beta_2^{(2)}}|^2 \equiv 1$ for all ℓ. Set the weights on V_2 as

$$
\omega_{2,[a]_{\mathcal{G}_2}} = 2, \quad \omega_{2,[c]_{\mathcal{G}_2}} = 3, \quad \omega_{2,[f]_{\mathcal{G}_2}} = 1.
$$

According to (8), we get $\boldsymbol{\varphi}_{2,[p]}$, $\boldsymbol{\psi}_{2,[p]}^{(1)}, \boldsymbol{\psi}_{2,[p]}^{(2)}$ as in Table 1.

(11) At level 1, set

$$
\widehat{\alpha_1}\left(\frac{\lambda_\ell}{\Lambda_2}\right) = \begin{cases} 1 & \ell = 1; \\ \frac{1}{\sqrt{2}} & \ell = 2; \\ 0 & \text{otherwise.} \end{cases} \quad \widehat{\beta_1^{(1)}}\left(\frac{\lambda_\ell}{\Lambda_2}\right) = \begin{cases} \frac{1}{\sqrt{2}} & \ell = 2; \\ \frac{1}{\sqrt{2}} & \ell = 3; \\ 0 & \text{otherwise.} \end{cases}
$$

Note that $|\widehat{\alpha_1}|^2 + |\widehat{\beta_1^{(1)}}|^2 = |\widehat{\alpha_2}|^2$ for all ℓ. Set the weights on V_1 as $\omega_{1,[a]_{\mathcal{G}_1}} = 2, \omega_{2,[c]_{\mathcal{G}_1}} = 4$. According to (8), we get $\boldsymbol{\varphi}_{1,[p]}$, $\boldsymbol{\psi}_{1,[p]}^{(1)}$ as in Table 2.

(12) At level 0, set

$$
\widehat{\alpha_0}\left(\frac{\lambda_\ell}{\Lambda_2}\right) = \begin{cases} 1 & \ell = 1; \\ 0 & \text{otherwise.} \end{cases} \quad \widehat{\beta_0^{(1)}}\left(\frac{\lambda_\ell}{\Lambda_2}\right) = \begin{cases} \frac{1}{\sqrt{2}} & \ell = 2; \\ 0 & \text{otherwise.} \end{cases}
$$

	a	b	c	d	e	f
$\boldsymbol{\varphi}_{2,[a]_{\mathcal{G}_2}}$	$\frac{1}{\sqrt{2}}$	$\frac{1}{\sqrt{2}}$	0	0	0	0
$\boldsymbol{\varphi}_{2,[c]_{\mathcal{G}_2}}$	0	0	$\frac{\sqrt{3}}{4}+\frac{\sqrt{6}}{24}$	$\frac{\sqrt{3}}{4}+\frac{\sqrt{6}}{24}$	$\frac{\sqrt{3}}{4}+\frac{\sqrt{6}}{24}$	$\frac{\sqrt{3}}{4}-\frac{\sqrt{6}}{8}$
$\boldsymbol{\varphi}_{2,[f]_{\mathcal{G}_2}}$	0	0	$\frac{1}{4}-\frac{\sqrt{2}}{8}$	$\frac{1}{4}-\frac{\sqrt{2}}{8}$	$\frac{1}{4}-\frac{\sqrt{2}}{8}$	$\frac{1}{4}+\frac{3\sqrt{2}}{8}$
$\boldsymbol{\psi}^{(1)}_{2,[a]_{\mathcal{G}_3}}$	0	0	0	0	0	0
$\boldsymbol{\psi}^{(1)}_{2,[b]_{\mathcal{G}_3}}$	0	0	0	0	0	0
$\boldsymbol{\psi}^{(1)}_{2,[c]_{\mathcal{G}_3}}$	0	0	$\frac{2}{3}+\frac{\sqrt{2}}{24}$	$-\frac{1}{3}+\frac{\sqrt{2}}{24}$	$-\frac{1}{3}+\frac{\sqrt{2}}{24}$	$-\frac{\sqrt{2}}{8}$
$\boldsymbol{\psi}^{(1)}_{2,[d]_{\mathcal{G}_3}}$	0	0	$-\frac{1}{3}+\frac{\sqrt{2}}{24}$	$\frac{1}{6}+\frac{7\sqrt{2}}{24}$	$\frac{1}{6}-\frac{5\sqrt{2}}{24}$	$-\frac{\sqrt{2}}{8}$
$\boldsymbol{\psi}^{(1)}_{2,[e]_{\mathcal{G}_3}}$	0	0	$-\frac{1}{3}+\frac{\sqrt{2}}{24}$	$\frac{1}{6}-\frac{5\sqrt{2}}{24}$	$\frac{1}{6}+\frac{7\sqrt{2}}{24}$	$-\frac{\sqrt{2}}{8}$
$\boldsymbol{\psi}^{(1)}_{2,[f]_{\mathcal{G}_3}}$	0	0	$-\frac{\sqrt{2}}{8}$	$-\frac{\sqrt{2}}{8}$	$-\frac{\sqrt{2}}{8}$	$\frac{3\sqrt{2}}{8}$
$\boldsymbol{\psi}^{(2)}_{2,[a]_{\mathcal{G}_3}}$	$\frac{1}{2}$	$-\frac{1}{2}$	0	0	0	0
$\boldsymbol{\psi}^{(2)}_{2,[b]_{\mathcal{G}_3}}$	$-\frac{1}{2}$	$\frac{1}{2}$	0	0	0	0
$\boldsymbol{\psi}^{(2)}_{2,[c]_{\mathcal{G}_3}}$	0	0	0	0	0	0
$\boldsymbol{\psi}^{(2)}_{2,[d]_{\mathcal{G}_3}}$	0	0	0	$\frac{\sqrt{2}}{4}$	$-\frac{\sqrt{2}}{4}$	0
$\boldsymbol{\psi}^{(2)}_{2,[e]_{\mathcal{G}_3}}$	0	0	0	$-\frac{\sqrt{2}}{4}$	$\frac{\sqrt{2}}{4}$	0
$\boldsymbol{\psi}^{(2)}_{2,[f]_{\mathcal{G}_3}}$	0	0	0	0	0	0

Table 1: Decimated framelets $\boldsymbol{\varphi}_{2,[p]_{\mathcal{G}_2}}, \boldsymbol{\psi}^{(1)}_{2,[p]_{\mathcal{G}_3}}, \boldsymbol{\psi}^{(2)}_{2,[p]_{\mathcal{G}_3}}$ at level $j=2$

.

	a	b	c	d	e	f
$\boldsymbol{\varphi}_{1,[a]_{\mathcal{G}_1}}$	$\frac{1}{3}+\frac{\sqrt{2}}{6}$	$\frac{1}{3}+\frac{\sqrt{2}}{6}$	$-\frac{1}{6}+\frac{\sqrt{2}}{6}$	$-\frac{1}{6}+\frac{\sqrt{2}}{6}$	$-\frac{1}{6}+\frac{\sqrt{2}}{6}$	$-\frac{1}{6}+\frac{\sqrt{2}}{6}$
$\boldsymbol{\varphi}_{1,[c]_{\mathcal{G}_1}}$	$\frac{1}{3}-\frac{\sqrt{2}}{6}$	$\frac{1}{3}-\frac{\sqrt{2}}{6}$	$\frac{1}{3}+\frac{\sqrt{2}}{12}$	$\frac{1}{3}+\frac{\sqrt{2}}{12}$	$\frac{1}{3}+\frac{\sqrt{2}}{12}$	$\frac{1}{3}+\frac{\sqrt{2}}{12}$
$\boldsymbol{\psi}^{(1)}_{1,[a]_{\mathcal{G}_2}}$	$\frac{1}{3}$	$\frac{1}{3}$	$-\frac{1}{6}$	$-\frac{1}{6}$	$-\frac{1}{6}$	$-\frac{1}{6}$
$\boldsymbol{\psi}^{(1)}_{1,[c]_{\mathcal{G}_2}}$	$-\frac{\sqrt{6}}{12}$	$-\frac{\sqrt{6}}{12}$	$\frac{\sqrt{6}}{12}$	$\frac{\sqrt{6}}{12}$	$\frac{\sqrt{6}}{12}$	$-\frac{\sqrt{6}}{12}$
$\boldsymbol{\psi}^{(1)}_{1,[f]_{\mathcal{G}_2}}$	$-\frac{\sqrt{2}}{12}$	$-\frac{\sqrt{6}}{12}$	$-\frac{\sqrt{2}}{12}$	$-\frac{\sqrt{2}}{12}$	$-\frac{\sqrt{2}}{12}$	$-\frac{5\sqrt{2}}{12}$

Table 2: Decimated framelets $\boldsymbol{\varphi}_{1,[p]_{\mathcal{G}_1}}, \boldsymbol{\psi}^{(1)}_{1,[p]_{\mathcal{G}_2}}$ at level $j=1$

.

	a	b	c	d	e	f
$\boldsymbol{\varphi}_{1,[a]_{\mathcal{G}_1}}$	$\frac{1}{6}$	$\frac{1}{6}$	$\frac{1}{6}$	$\frac{1}{6}$	$\frac{1}{6}$	$\frac{1}{6}$
$\boldsymbol{\psi}^{(1)}_{1,[a]_{\mathcal{G}_2}}$	$\frac{1}{3}$	$\frac{1}{3}$	$-\frac{1}{6}$	$-\frac{1}{6}$	$-\frac{1}{6}$	$-\frac{1}{6}$
$\boldsymbol{\psi}^{(1)}_{1,[c]_{\mathcal{G}_2}}$	$-\frac{\sqrt{2}}{6}$	$-\frac{\sqrt{2}}{6}$	$\frac{\sqrt{2}}{12}$	$\frac{\sqrt{2}}{12}$	$\frac{\sqrt{2}}{12}$	$\frac{\sqrt{2}}{12}$

Table 3: Decimated framelets $\boldsymbol{\varphi}_{0,[p]_{\mathcal{G}_0}}, \boldsymbol{\psi}^{(1)}_{0,[p]_{\mathcal{G}_1}}$ at level $j=0$

.

Note that $|\widehat{\alpha_0}|^2+|\widehat{\beta_0^{(1)}}|^2=|\widehat{\alpha_1}|^2$ for all ℓ. Set the weights on V_0 as $\omega_{1,[a]_{\mathcal{G}_0}}=6$. According to (8), we get $\boldsymbol{\varphi}_{0,[p]}$, $\boldsymbol{\psi}^{(1)}_{0,[p]}$ as in Table 3.

It is easy to check that conditions in (15) and (16) hold. Hence, by Theorem 2.1 the decimated framelet system

$$\{\boldsymbol{\varphi}_{J_1,[p]} : [p]\in V_{J_1}\}\cup\{\boldsymbol{\psi}^{(n)}_{j,[p]} : [p]\in V_{j+1},\ j=J_1,\ldots,J\}$$

constructed through the above steps (1)–(12) is a decimated tight frame for $L_2(\mathcal{G})$ for all $J_1=0,1,2,3$.

ACKNOWLEDGMENTS

The research of X. Zhuang and the work described in this paper was partially supported by a grant from the Research Grants Council of the Hong Kong Special Administrative Region, China (Project No. CityU 11300717).

REFERENCES

[1] Meyer, Y., [*Ondelettes et opérateurs. I*], Actualités Mathématiques. [Current Mathematical Topics], Hermann, Paris (1990).

[2] Chui, C. K., [*An introduction to wavelets*], vol. 1 of *Wavelet Analysis and its Applications*, Academic Press, Inc., Boston, MA (1992).

[3] Daubechies, I., [*Ten lectures on wavelets*], vol. 61 of *CBMS-NSF Regional Conference Series in Applied Mathematics*, Society for Industrial and Applied Mathematics (SIAM), Philadelphia, PA (1992).

[4] Mallat, S., [*A wavelet tour of signal processing. The sparse way, With contributions from Gabriel Peyré*], Elsevier/Academic Press, Amsterdam, Third ed. (2009).

[5] Han, B., [*Framelets and Wavelets: Algorithms, Analysis, and Applications*], Birkhäuser (2017).

[6] Singer, A., "From graph to manifold laplacian: The convergence rate," *Applied and Computational Harmonic Analysis* **21**(1), 128 – 134 (2006). Special Issue: Diffusion Maps and Wavelets.

[7] Belkin, M., Matveeva, I., and Niyogi, P., "Regularization and semi-supervised learning on large graphs," in [*Learning Theory*], Shawe-Taylor, J. and Singer, Y., eds., 624–638, Springer Berlin Heidelberg, Berlin, Heidelberg (2004).

[8] Bronstein, M. M., Bruna, J., LeCun, Y., Szlam, A., and Vandergheynst, P., "Geometric deep learning: Going beyond euclidean data," *IEEE Signal Processing Magazine* **34**, 18–42 (July 2017).

[9] Fawzi, A., Moosavi-Dezfooli, S.-M., Frossard, P., and Soatto, S., "Empirical study of the topology and geometry of deep networks," in [*The IEEE Conference on Computer Vision and Pattern Recognition (CVPR)*], 3762–3770 (2018).

[10] Merriman, B., Bence, J. K., and Osher, S., "Diffusion generated motion by mean curvature," in [*Computational Crystal Growers Workshop*], Taylor, J., ed., 73–83, American Mathematical Society, Providence, Rhode Island (1992).

[11] Bertozzi, A. L. and Flenner, A., "Diffuse interface models on graphs for classification of high dimensional data," *Multiscale Modeling & Simulation* **10**(3), 1090–1118 (2012).

[12] Garcia-Cardona, C., Merkurjev, E., Bertozzi, A. L., Flenner, A., and Percus, A., "Multiclass data segmentation using diffuse interface methods on graphs," *IEEE Transactions on Pattern Analysis and Machine Intelligence* **36**(8), 1600–1613 (2014).

[13] Coifman, R. R., Lafon, S., Lee, A. B., Maggioni, M., Nadler, B., Warner, F., and Zucker, S. W., "Geometric diffusions as a tool for harmonic analysis and structure definition of data: Diffusion maps," *Proceedings of the National Academy of Sciences* **102**(21), 7426–7431 (2005).

[14] Dongen, S., "A cluster algorithm for graphs," tech. rep., Amsterdam (2000).

[15] Gavish, M. and Coifman, R. R., "Sampling, denoising and compression of matrices by coherent matrix organization," *Applied and Computational Harmonic Analysis* **33**(3), 354 – 369 (2012).

[16] Gavish, M., Nadler, B., and Coifman, R. R., "Multiscale wavelets on trees, graphs and high dimensional data: Theory and applications to semi supervised learning.," in [*Proceedings of the 27th International Conference on Machine Learning (ICML)*], 367–374 (2010).

[17] Lafon, S. and Lee, A. B., "Diffusion maps and coarse-graining: A unified framework for dimensionality reduction, graph partitioning, and data set parameterization," *IEEE Transactions on Pattern Analysis and Machine Intelligence* **28**(9), 1393–1403 (2006).

[18] Chui, C. K., Mhaskar, H., and Zhuang, X., "Representation of functions on big data associated with directed graphs," *Applied and Computational Harmonic Analysis* **44**(1), 165–188 (2018).

[19] Maggioni, M. and Mhaskar, H. H., "Diffusion polynomial frames on metric measure spaces," *Applied and Computational Harmonic Analysis* **24**(3), 329 – 353 (2008).

[20] Bodmann, B., Kutyniok, G., and Zhuang, X., "Gabor shearlets," *Applied and Computational Harmonic Analysis* **38**, 87–114 (1 2015).

[21] Han, B., "Nonhomogeneous wavelet systems in high dimensions," *Applied and Computational Harmonic Analysis* **32**(2), 169–196 (2012).

[22] Han, B. and Zhuang, X., "Smooth affine shear tight frames with mra structure," *Applied and Computational Harmonic Analysis* **39**, 300–338 (9 2015).

[23] Zhuang, X., "Digital affine shear transforms: fast realization and applications in image/video processing," *SIAM Journal on Imaging Sciences* **9**(3), 1437–1466 (2016).

[24] Wang, Y. G. and Zhuang, X., "Tight framelets and fast framelet filter bank transforms on manifolds," *Applied and Computational Harmonic Analysis* (2018).

[25] Ron, A. and Shen, Z., "Affine systems in $L_2(R^d)$: The analysis of the analysis operator," *Journal of Functional Analysis* **148**(2), 408 – 447 (1997).

[26] Daubechies, I., Han, B., Ron, A., and Shen, Z., "Framelets: Mra-based constructions of wavelet frames," *Applied and Computational Harmonic Analysis* **14**(1), 1 – 46 (2003).